

Synthesis, Characterization, and Application in Asymmetric Hydrogenation Reactions of Chiral Ruthenium(II) Diphosphine Complexes

Nadia C. Zanetti,[†] Felix Spindler,^{*,‡} John Spencer,[†] Antonio Togni,^{*,†} and Greta Rihs[‡]

Central Research Services, FD 6, Ciba-Geigy Ltd., P.O. Box, CH-4002 Basel, Switzerland, and Laboratory of Inorganic Chemistry, Swiss Federal Institute of Technology, ETH-Zentrum, CH-8092 Zurich, Switzerland

Received August 30, 1995[®]

Four new complexes of the type $[\text{Ru}(\text{CF}_3\text{CO}_2)_2(\text{X})_2(\text{PP})]$ **7** (X = methanol or ethanol, PP = chiral diphosphine) have been synthesized from the reaction of PP with $[\text{Ru}_2(\text{CF}_3\text{CO}_2)_4(\text{H}_2\text{O})_2(\text{COD})_2]$ and characterized by both NMR spectroscopy and single-crystal X-ray diffraction studies. A common feature of these complexes is a pseudooctahedral geometry for ruthenium, an unusual monodentate ligation mode for the mutually *trans* trifluoroacetate groups, along with two solvent molecules coordinated in mutual *cis* positions (MeOH for **7a** and **7b**, EtOH for **7c**). **7a** (PP = (2*S*,4*S*)-BDPP) belongs to the orthorhombic $P2_12_12_1$ space group, $Z = 4$, $a = 9.896(1)$ Å, $b = 19.099(3)$ Å, and $c = 19.689(2)$ Å. **7b** (PP = (4*S*,5*S*)-DIOP) also crystallizes in the orthorhombic $P2_12_12_1$ space group, $Z = 4$, $a = 12.679(1)$ Å, $b = 16.744(2)$ Å, and $c = 18.944(2)$ Å. **7c** (PP = (*R*)-1-[(*S*)-2-(diphenylphosphino)ferrocenyl]ethylidicyclohexylphosphine, abbreviated as PPF₂Cy₂) belongs to the monoclinic $P2_1$ space group, $Z = 4$, $a = 18.153(2)$ Å, $b = 12.364(2)$ Å, $c = 20.431(1)$ Å, and $\beta = 97.40(1)^\circ$. The air-stable $[\text{RuCl}_2(p\text{-cymene})(\text{PP})]\text{PF}_6$ **9** were synthesized from the reaction of PP with $[\text{RuCl}_2(p\text{-cymene})]_2$ in a refluxing $\text{CH}_2\text{Cl}_2/\text{EtOH}$ mixture, followed by metathesis with KPF_6 in MeOH, in 72–89% yields (PP = (*S*)-(*R*) or (*R*)-(*S*)-2-(diphenylphosphino or arsino)ferrocenyl]ethylbisphosphine derivative). **9a** (PP = (*S*)-(*R*)-PPF₂Cy₂) crystallizes in the monoclinic space group $P2_1$, $Z = 2$, $a = 11.965(2)$ Å, $b = 14.852(3)$ Å, $c = 13.999(2)$ Å, and $\beta = 111.50(2)^\circ$. Complexes **7** were probed for their catalytic behavior in the hydrogenation of methyl acetamidocinnamate **10**, acetamidocinnamic acid **11**, and dimethyl itaconate **12**. Using a typical substrate to catalyst ratio of 50–100:1 and $p(\text{H}_2) = 50$ bar, modest enantiomeric excesses (ee) of up to 75% were achieved. The highest ee's were attained in CH_2Cl_2 or a 5:4 THF/ CH_2Cl_2 mixture, whereas higher activities were observed when methanol was employed as solvent. The addition of NEt_3 had a beneficial effect on the ee of the reactions involving **11**, whereas with **10** a detrimental effect was observed. The reactions involving **12** gave poor enantioselectivity.

Introduction

Recent years have witnessed increasingly impressive catalytic applications of ruthenium(II) diphosphine complexes in asymmetric hydrogenation reactions with notable developments including their successful employment in the formation of highly enantiomerically enriched alcohols from ketone, lactone, or ester precursors and their use in olefin hydrogenation.^{1–3} In this respect, structurally well-characterized complexes incorporating atropisomeric biarylphosphines (PP) of the

type $[\text{Ru}(\text{RCO}_2)_2(\text{PP})]$ (PP = BINAP (**I**),¹ BIPHEMP (**II**)²) have given excellent results, although there would still appear to be a definite lack of well-characterized, analogous complexes containing different phosphine backbones (see Chart 1).³

We recently embarked on a project aimed at preparing a series of dicarboxylate and η^6 -aryl-bound ruthenium(II) complexes, containing phosphines other than **I** or **II**, for structural characterization and evaluation of their catalytic properties. Ligands **III**,⁴ **IV**,⁵ **V**,⁶ **1**,⁷ and **2**,⁸ as well as a whole host of ferrocenyl bisphosphines **3–5**, and one arsenylphosphine **3d**, were appropriate candidates for the attempted synthesis of the required

[†] ETH-Zentrum.

[‡] Central Research Services, Ciba-Geigy Ltd.

[®] Abstract published in *Advance ACS Abstracts*, December 15, 1995.

(1) (a) For an excellent overview, see: Takaya, H.; Ohta, T.; Noyori, R. In *Catalytic Asymmetric Synthesis*; Ojima, I., Ed.; VCH Publishers: New York, 1993; pp 1–39, and references cited therein. (b) Noyori, R.; Takaya, H. *Acc. Chem. Res.* **1990**, *23*, 345. (c) Takaya, H.; Ohta, T.; Mashima, K.; Noyori, R. *Pure Appl. Chem.* **1990**, 1135. (d) Mashima, K.; Kusano, K.; Sato, N.; Matsumura, Y.; Nozaki, K.; Kumobayashi, H.; Sayo, N.; Hori, Y.; Ishizaki, T.; Akutagawa, S.; Takaya, H. *J. Org. Chem.* **1994**, *59*, 3064. (e) Ohta, T.; Miyake, T.; Seido, N.; Kumobayashi, H.; Takaya, H. *J. Org. Chem.* **1995**, *60*, 357.

(2) (a) Schmid, R.; Cereghetti, M.; Heiser, B.; Schönholzer, P.; Hansen, H. *J. Helv. Chim. Acta* **1988**, *71*, 897. (b) Heiser, B.; Broger, E. A.; Cramer, Y. *Tetrahedron: Asymmetry* **1991**, *2*, 51. (c) Mezzetti, A.; Tschumper, A.; Consiglio, G. *J. Chem. Soc., Dalton Trans.* **1995**, 49.

(3) (a) Genet, J. P.; Mallart, S.; Pinel, C.; Juge, S.; Laffitte, J. A. *Tetrahedron: Asymmetry* **1991**, *2*, 43. (b) Alcock, N. W.; Brown, J. M.; Rose, M.; Wienaud, A. *Tetrahedron: Asymmetry* **1991**, *2*, 47. (c) James, B. R.; Dang, D. K. W. *Can. J. Chem.* **1980**, *58*, 245. (d) Kawano, H.; Ikariya, T.; Ishii, Y.; Kodama, T.; Saburi, M.; Yoshikawa, S.; Uchida, Y.; Akutagawa, S. *Bull. Chem. Soc. Jpn.* **1992**, *65*, 1595.

(4) (a) Achiwa, K. *J. Am. Chem. Soc.* **1976**, *98*, 8265. (b) Ojima, I.; Yoda, N. *Tetrahedron Lett.* **1980**, *21*, 1051.

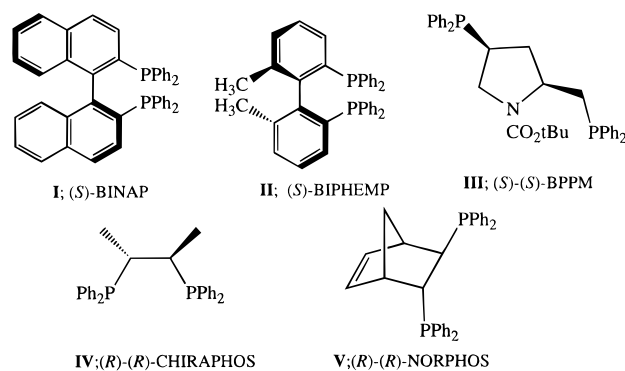
(5) Fryzuk, M. D.; Bosnich, B. *J. Am. Chem. Soc.* **1977**, *99*, 6262.

(6) Brunner, H.; Pieronczyk, W.; Schönhammer, B.; Streng, K.; Bernal, I.; Korp, J. *Chem. Ber.* **1981**, *114*, 1137.

(7) McNeil, P. A.; Roberts, N. K.; Bosnich, B. *J. Am. Chem. Soc.* **1981**, *103*, 2280.

(8) Kagan, H. B.; Dang, T. P. *J. Am. Chem. Soc.* **1972**, *94*, 6429.

Chart 1

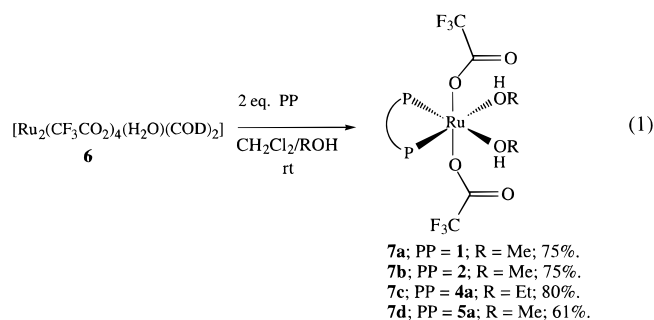


complexes (see Chart 2). The choice of ligands such as **3**, **4**, and **5** was especially desirable given their current high scope of application in many different catalytic reactions.^{9,10} Moreover, the myriad of structural permutations possible by simple chemical transformations at the stereogenic side arm renders these ferrocenyl systems very attractive for a study of both steric and electronic effects in catalysis.¹⁰ Compounds **5**¹¹ have the added complexity of containing a third, further stereogenic center *viz.* the phosphorus atom.

This study has resulted in the formation of a series of complexes of the type $[\text{Ru}(\text{CF}_3\text{CO}_2)_2(\text{X})_2(\text{PP})]$ and $[\text{RuCl}(\textit{p}\text{-cymene})(\text{PP})]\text{PF}_6$ where X = methanol or ethanol, and PP a chiral diphosphine (See Chart 2). The characterization of such complexes by NMR, X-ray analyses, and preliminary results pertaining to their use in the catalytic hydrogenation of various olefinic derivatives will be presented hereafter.

Results and Discussion

Synthesis of 7. The addition of an equimolar amount of a dichloromethane solution of the phosphines **1**, **2**, **4a**, or **5a** to a stirred solution of $[\text{Ru}_2(\text{CF}_3\text{CO}_2)_4(\text{H}_2\text{O})(\text{COD})_2]$ **6** (COD = 1,5-cyclooctadiene) in methanol or ethanol at room temperature afforded, after workup, the yellow or red complexes $[\text{Ru}(\text{CF}_3\text{CO}_2)_2(\text{ROH})_2(\text{PP})]$ **7** in high yields (eq 1). These solids can be



stored under argon at rt but are rather air-sensitive in solution, turning green. Attempts at extending this

(9) (a) Hayashi, T. In *Ferrocenes*; Togni, A., Hayashi, T., Eds.; VCH Publishers: New York, 1995; Chapter 2, p 105, and references cited therein. (b) Hayashi, T. *Pure Appl. Chem.* **1988**, *60*, 7.

(10) (a) Togni, A.; Breutel, C.; Schnyder, A.; Spindler, F.; Landert, H. *J. Am. Chem. Soc.* **1994**, *116*, 4062. (b) Schnyder, A.; Hintermann, L.; Togni, A. *Angew. Chem.* **1995**, *34*, 931. (c) Abbenhuis, H. C. L.; Burckhardt, U.; Gramlich, V.; Köllner, C.; Pregosin, P.; Salzmann, R.; Togni, A. *Organometallics* **1995**, *14*, 759.

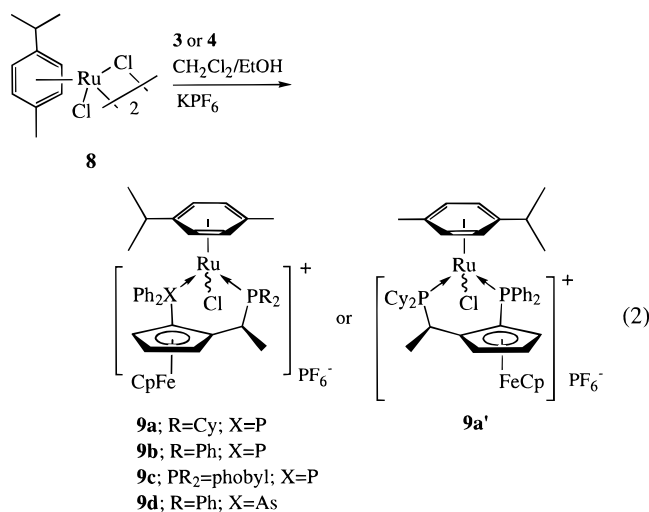
(11) Togni, A.; Breutel, C.; Soares, M.; Zanetti, N.; Gerfin, T.; Gramlich, V.; Spindler, F.; Rihs, G. *Inorg. Chim. Acta* **1994**, *222*, 213.

(12) Albers, M. O.; Liles, D. C.; Singleton, E.; Yates, J. E. *J. Organomet. Chem.* **1984**, *272*, C62.

synthetic route to ligands **III–V** were unfortunately unsuccessful as were the reactions of the same phosphines with $[\text{RuCl}_2(\text{COD})]_n$ in the presence of a base.^{3d,13a} Ligands **4b**, **4c**, **5b**, and **5c** were reacted *in situ* with **6** in MeOH at rt for 1 h, and after solvent removal *in vacuo*, the resulting yellow powders were used directly in the hydrogenation reactions (*vide infra*).

The structures of **7** in solution were probed by ³¹P NMR spectroscopy. Complexes **7a** and **7b**, consistent with the C₂ symmetry axis passing through the two phosphorus atoms, perpendicular to the CF₃CO₂Ru bond, gave singlets in their ³¹P NMR spectrum, the chemical shift of the homotopic phosphorus atoms being shifted downfield with respect to the starting ligands. Despite the two complexes having diarylalkylphosphine backbones, the ³¹P chemical shift of **7a** ($\delta = 62.7$ ppm in CDCl₃) is almost 20 ppm downfield from that of **7b** ($\delta = 45.4$ ppm). As expected, **7c** and **7d** gave AB systems due to the nonequivalence of the P atoms. On the basis of the ¹H NMR spectra it was not possible to distinguish between a bidentate or monodentate coordination mode of the trifluoroacetate ligand in **7**. Moreover, there was no observable difference in chemical shift between coordinated and free methanol, indicating a fast exchange process.

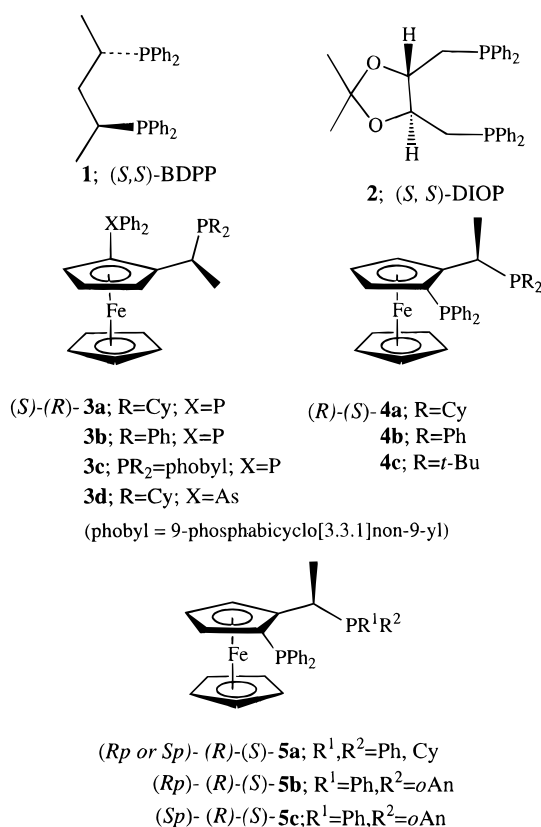
Synthesis of 9. The reaction of **3** or **4** with $[\text{RuCl}_2(\textit{p}\text{-cymene})_2]$ **8** in a CH₂Cl₂/EtOH mixture, followed by metathesis with KPF₆ in MeOH furnished, after workup, the cationic, air-stable solids **9** (eq 2). Analysis of



the ³¹P NMR spectra of **9** was most informative, and varying degrees of diastereoselectivity were observed depending on the phosphine ligand used. Since the ruthenium atom in complexes **9** is now a new stereogenic center, two possible diastereomeric forms arise. Whereas the ³¹P NMR spectrum of **9a** displayed one major AB system (diastereoselectivity ~15:1, with a ²J_{PP} = 55.8 Hz between the PCy₂ and PPh₂ groups), that of **9b** presented two such AB systems in a ~5:1 ratio (²J_{PP} = 58.8 Hz between the two PPh₂ groups). This latter distribution of diastereomers most likely represents the thermodynamic product ratio of the reaction, since refluxing a further 16 h under the same reaction conditions led to no change in this ratio, by ³¹P NMR.

(13) (a) Ohta, T.; Takaya, H.; Noyori, R. *Inorg. Chem.* **1988**, *27*, 566. (b) For an overview of bonding modes of carboxylate complexes, see: Rardin, R. L.; Tolman, W. B.; Lippard, S. J. *New. J. Chem.* **1991**, *15*, 417.

Chart 2



The ³¹P NMR spectrum of **9d** displayed, as expected, a singlet for the PPh₂ group whereas that of **9c** was rather complicated, with a broad multiplet at $\delta = \sim 35$ ppm and a sharp doublet at $\delta = 29$ ppm. This can be explained by a rapid exchange process between the arene group and the Cl atom on the NMR time scale. **9c** proved, moreover, to be rather difficult to obtain in pure form.

Structural Characterization of 7a–c and 9a. In order to elucidate the precise bonding mode of the trifluoroacetate groups and the overall geometry of the complexes in the solid state, single-crystal structure determinations of **7a–c** were carried out. Crystals of **7a** and **7b** suitable for such a determination were obtained by recrystallization in MeOH and those of **7c** from EtOH. Crystallographic data are given in Table 1. A selection of bond lengths and angles for complexes **7a–c** is shown in Table 2.

The Shabal plots given in Figure 1 show, common for each of these three complexes, a near-octahedral geometry for ruthenium and mutually *trans* ligated monodentate trifluoroacetate groups, along with two solvent molecules coordinated in mutual *cis* positions (MeOH for **7a** and **7b**, EtOH for **7c**). The bite angles (P–Ru–P) found for **7a** and **7b** are 92.3 and 94.7°, respectively (see Table 2), which are somewhat larger than the 90.6(1)° found for [Ru(OCOt-Bu)₂(BINAP)].^{13a} **7c** comprised two independent molecules in the unit cell.

The most striking feature of these structures is the monodentate ligation of the trifluoroacetate groups to ruthenium, which is in sharp contrast to an analogous BINAP–Ru complex in which this ligand adopts a bidentate bonding mode.¹³ The relatively low basicity, and hence weak *trans* influence, of the BINAP ligand as compared to the higher alkylated phosphines in **7a–c**

may be a contributing factor to this structural difference. The stability of **7a–c** can be attributed to the formation of two relatively strong hydrogen bonds¹⁴ between the carbonyl groups of the trifluoroacetate ligands and the protons of the coordinated solvent molecules (O···O distances between 2.5 and 2.7 Å), a feature that is not without precedent in ruthenium chemistry.¹⁵

The structure of **9a** was also determined, of crystals obtained by slow diffusion of diethyl ether into a dichloromethane solution at room temperature (Figure 2). The ruthenium atom is part of an overall piano stool arrangement, comprising the η^6 -bound cymene group, the chloride ion, and the two distinct phosphine atoms of the ferrocenyl ligand. The P–Ru distances corresponding to the aryl (P1) and alkyl (P2) phosphines in the six-membered ruthenacycle are slightly different, P1–Ru being 2.368(2) Å and P2–Ru 2.390(2) Å. Other distances, e.g., Ru–Cl (2.400 Å), fall in the normal range. The bite angle (P–Ru–P) of 92.6(1)° is slightly larger than that of the related [RuCl(benzene)((*S*)-BINAP)] complex^{1c,16} (P–Ru–P = 91.4(1)°) and that of **7c** (90.5°). The P1–Ru–Cl and P2–Ru–Cl angles of 85.1(1)° and 85.9°, respectively, emphasize the distorted *fac*-octahedral geometry of the complex (see Table 3).

Hydrogenation Reactions. The catalytic activity of mainly **7** in the enantioselective hydrogenation of the olefinic substrates **10–12** was examined, preliminary results obtained with **9a** and **9d** being very disappointing (enantiomeric excesses (ee's) and conversions of $\sim 10\%$ with **10** as substrate after ~ 17 h) and not pursued further. Substrate/catalyst ratios of either 50 or 100 were routinely employed, and the results are compiled in Table 4, including those obtained using the *in situ* generated complexes [Ru(CF₃CO₂)₂(MeOH)₂(PP)], where PP = **4b**, **4c**, **5b**, and **5c**.

A few pertinent conclusions can be drawn from these results. First, a strong solvent effect on enantioselectivity is apparent. The enantioselectivity is clearly higher in aprotic (CH₂Cl₂ or THF) than in protic solvents (MeOH) and such an effect is rather pronounced when substrates **10** and **11** are employed. Thus, **10** was hydrogenated in the presence of **7a** as catalyst with an ee of 69% in CH₂Cl₂, whereas in MeOH the ee was significantly lower (24%) (entries 1 and 2, Table 4). With the same catalyst, **11** was hydrogenated in a 5:4 mixture of THF/CH₂Cl₂ with an ee of 47% whereas in MeOH only a 3% ee was observed (entries 4 and 5). Similarly, again in the hydrogenation of **10**, with the *in situ*-generated complex obtained from **6** and **5b**, the ee dropped in changing from CH₂Cl₂ (75% ee) to MeOH (31% ee) (entries 14 and 15). A similar decrease in enantioselectivity by the same change in solvent has already been reported for the hydrogenation of various carbonyl functions,^{17,18} whereas the opposite

(14) Emsley, J. *Chem. Soc. Rev.* **1980**, 9, 91.

(15) (a) Dobson, A.; Moore, D. S.; Robinson, S. D.; Hursthouse, M. B.; New, L. *Polyhedron* **1985**, 4, 1119. (b) Albers, M. O.; Liles, D. C.; Singleton, E. *Acta Crystallogr.* **1987**, C43, 860.

(16) Mashima, K.; Kusano, K.; Ohta, T.; Noyori, R.; Takaya, H. *J. Chem. Soc., Chem. Commun.* **1989**, 1208.

(17) Genet, J. P.; Pinel, C.; Mallart, S.; Juge, S.; Thorimbert, S.; Laffitte, J. A. *Tetrahedron: Asymmetry* **1991**, 2, 555.

(18) Mashima, K.; Matsumura, Y.; Kusano, K.; Kumobayashi, H.; Sayo, N.; Hori, Y.; Ishizaki, T.; Akutagawa, S.; Takaya, H. *J. Chem. Soc., Chem. Commun.* **1991**, 609.

Table 1. Structural Parameters for 7a–c and 9a

compound	7a	7b	7c	9a
formula	C ₃₅ H ₃₈ O ₆ F ₆ P ₂ Ru	C ₃₇ H ₃₂ D ₈ O ₈ F ₆ P ₂ Ru	C ₄₄ H ₅₄ O ₆ F ₆ P ₂ RuFe	C ₄₆ H ₅₈ ClF ₆ P ₃ RuFe
mol wt	831.69	897.78	1011.76	1010.2
crystal dimens (mm)	0.70 × 0.45 × 0.36	0.76 × 0.60 × 0.30	0.54 × 0.31 × 0.10	0.8 × 0.6 × 0.45
cryst syst	orthorhombic	orthorhombic	monoclinic	monoclinic
space group	P2 ₁ 2 ₁ 2 ₁	P2 ₁ 2 ₁ 2 ₁	P2 ₁	P2 ₁
a (Å)	9.896(1)	12.679(1)	18.153(2)	11.965(2)
b (Å)	19.099(3)	16.744(2)	12.364(2)	14.852(3)
c (Å)	19.689(3)	18.944(2)	20.431(1)	13.999(2)
β(°)			97.40(1)	111.50(2)
V(Å ³)	3721(1)	4022(1)	4547(1)	2314.6(7)
Z	4	4	4	2
ρ (calcd) (g·cm ⁻³)	1.484	1.483	1.478	1.449
μ (cm ⁻¹)	4.90	5.325	7.78	8.56
F(000)	1696	1816	2080	1040
diffractometer	Enraf-Nonius CAD4	Phillips PW1100	Phillips PW1100	Syntex P21
radiation (graph. monoch)	Cu Kα	Mo Kα	Mo Kα	Mo Kα
2θ range (deg)	6–150	6–60	6–60	3–40
no. of unique reflcns	4308	6508	14271	2433
no. of obsd reflcns (n _b)	4277	4065	5670	2287
refinement methods	full matrix	full matrix	full matrix (in 2 blocks)	full matrix
hydrogen atoms	not located	not located	not located	Riding model; fixed isotr U
no. of params	451	487	1080	517
R	0.069	0.064	0.036	0.027
R _w	0.079	0.076	0.042	0.034

Table 2. Selected Bond Distances (Å) and Angles (deg) for 7a–c

Bond Distances for 7a			
Ru–P2	2.255(4)	O13–O15	2.658
Ru–P3	2.252(4)	Ru–O10	2.11(1)
Ru–O12	2.16(1)	Ru–O14	2.18(1)
Ru–O15	2.23(1)	O11–O14	2.675
Bond Angles for 7a			
P2–Ru–P3	92.3(1)	P2–Ru–O10	100.0(3)
P2–Ru–O15	173.0(2)	P3–Ru–O10	91.4(3)
P3–Ru–O12	94.7(3)	P3–Ru–O14	175.2(3)
P3–Ru–O15	94.4(2)	P2–Ru–O14	92.5(3)
Bond Distances for 7b			
Ru–P2	2.248(3)	Ru–P3	2.253(3)
Ru–O14	2.104(8)	Ru–O12	2.107(8)
Ru–O17	2.234(9)	Ru–O16	2.202(9)
O15–O17	2.62(1)	O13–O16	2.57(1)
Bond Angles for 7b			
P2–Ru–P3	94.7(1)	P2–Ru–O12	92.4(3)
P2–Ru–O14	87.9(3)	P2–Ru–O16	93.8(3)
P2–Ru–O17	174.6(2)	P3–Ru–O12	90.8(2)
P3–Ru–O14	94.3(3)	P3–Ru–O16	171.4(3)
P3–Ru–O17	90.2(2)		
Bond Distances for 7c			
Ru–P5	2.296(3)	Ru–P6	2.256(3)
Ru–O21	2.114(7)	Ru–O23	2.133(7)
Ru–O25	2.220(7)	Ru–O26	2.232(7)
O13–O16	2.63	O15–O17	2.56
Bond Angles for 7c			
P5–Ru–P6	90.5(1)	P5–Ru–O21	88.6(2)
P5–Ru–O23	94.9(2)	P5–Ru–O25	94.5(2)
P6–Ru–O21	91.6(2)	P6–Ru–O23	93.5(2)
P6–Ru–O25	175.0(2)	P6–Ru–O26	90.5(2)

trend was observed using [RuBr₂((R)-BINAP)] as catalyst for the hydrogenation of **10**, the ee increasing in changing from CH₂Cl₂ (24% ee) to methanol (85% ee) as solvent.¹⁹

The activity of all catalysts investigated is higher in MeOH than in CH₂Cl₂. The hydrogenation of **10**, catalyzed by **7c**, was complete within 0.1 h (entry 13), whereas in CH₂Cl₂, only 34% conversion was attained after 18 h (entry 12). The optical yields of these two reactions were both, however, very low. Using the *in situ*-generated complexes [Ru(CF₃CO₂)₂(MeOH)₂(PP)]

where PP = **5b**, for the hydrogenation of **10**, a yield of 29%, and an ee of 57% was obtained in CH₂Cl₂ whereas in MeOH, after only 4 h, quantitative conversion was achieved, the ee being, however, only 30% (entries 20 and 21, respectively). Here, a substrate/catalyst ratio of 100:1 was employed. Other *in situ*-generated catalysts, from **4b** and **4c**, for example, (entries 22 and 23) gave poor results, even with a substrate/catalyst ratio of 50:1.

In the hydrogenation of **10** and **11**, both the enantioselectivity and activity of the catalyst were influenced by the addition of NEt₃. The addition of base increased the optical yield of product for the hydrogenation of **11** in both protic and aprotic solvents (compare entries 6 and 5 and entries 7 and 4), whereas the optical yield observed for the hydrogenation of **10**, in the presence of **7a** or **7c**, diminished upon addition of base (entries 1 and 3, where the ee decreases from 69 to 29%). Such a pronounced effect by the addition of base observed for **11** may be due to an acceleration of the heterolytic hydrogen activation and the generation of a carboxylate group which would be able to coordinate to ruthenium. This would decrease the number of degrees of freedom of the system, in terms of coordination geometry, and thus contribute to achieving a higher enantiodiscrimination.²⁰

The extra, phosphorus stereogenic center in **5b** (P has the *R* configuration) and **5c** (P has the *S* configuration) allows for a study of the effect of chirality at phosphorus on the enantioselectivity of the hydrogenation process.²¹ In the hydrogenation of **10**, carried out in CH₂Cl₂, the *in situ*-generated complexes [Ru(CF₃CO₂)₂(MeOH)₂(PP)], where PP = **5b** or **5c**, gave significantly different results, the activity and enantioselectivity of the reactions being higher (74% ee, 85% yield) when complex **5b** (entry 14) was employed as opposed to the 57% ee, and 29% yield, obtained for the complex incorporating **5c** (entry 20). Despite the different absolute configuration at the stereogenic P atom, the reactions catalyzed by **5b** and **5c** afforded the *R*-enriched products, a

(19) Noyori, R.; Ikeda, T.; Ohkuma, T.; Widhalm, M.; Kitamura, M.; Takaya, H.; Akutagawa, S.; Sayo, N.; Saito, T.; Taketomi, T.; Kumobayashi, H. *J. Am. Chem. Soc.* **1989**, *111*, 9134.

(20) Ashby, M. T.; Halpern, J. *J. Am. Chem. Soc.* **1991**, *113*, 589.
(21) (a) Nagel, U.; Rieger, B. *Organometallics* **1989**, *8*, 1534. (b) Nagel, U.; Bublewitz, A. *Chem. Ber.* **1992**, *125*, 1061.

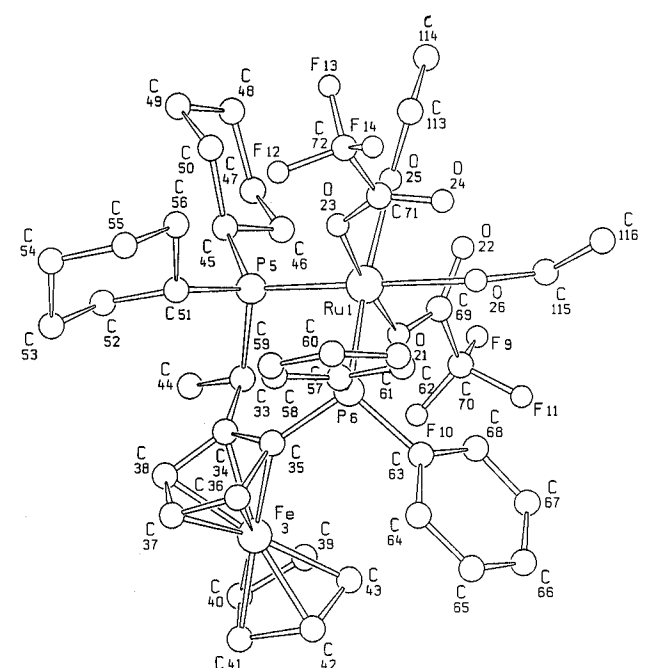
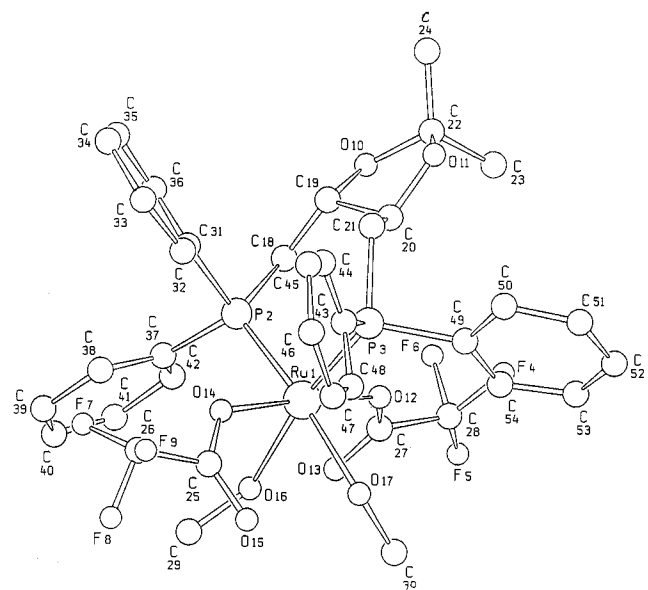
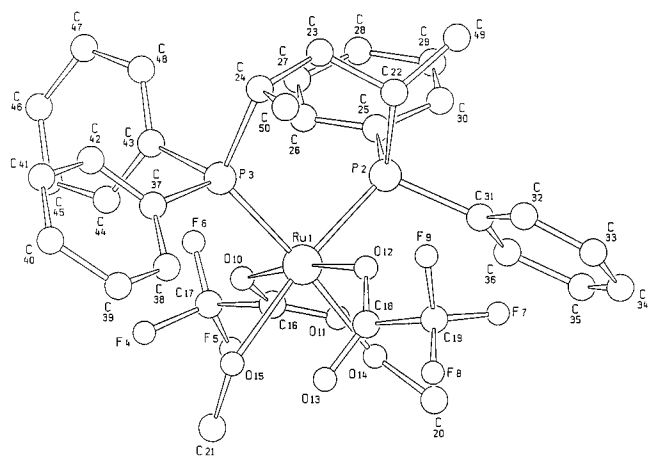


Figure 1. Schakal views of the complexes (top) $[\text{Ru}(\text{CF}_3\text{CO}_2)_2(\text{MeOH})_2(2S,4S)\text{-BDPP}]$ (**7a**), (middle) $[\text{Ru}(\text{CF}_3\text{CO}_2)_2(\text{MeOH})_2(4S,5S)\text{-DIOP}]$ (**7b**), and (bottom) $[\text{Ru}(\text{CF}_3\text{CO}_2)_2(\text{EtOH})_2(R)\text{-}(S)\text{-PPFCy}_2]$ (**7c**).

result in line with previous observations in analogous Rh chemistry.^{15a}

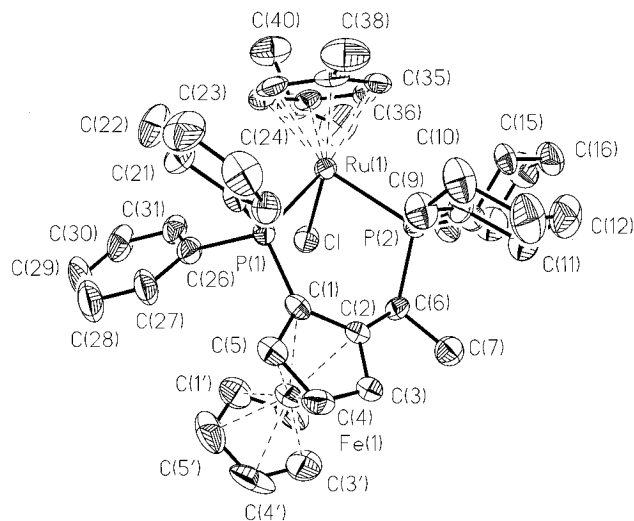


Figure 2. ORTEP view of **9a'**.

Table 3. Selected Bond Distances (Å) and Angles (deg) for **9a'**

Bond Distances			
Ru–Cl	2.400(2)	Ru–P2	2.390(2)
Ru–P1	2.368(2)	Ru–C32	2.270(8)
Ru–C33	2.238(8)	Ru–C34	2.272(8)
Ru–C35	2.224(8)	Ru–C36	2.273(8)
Ru–C37	2.321(8)		
Bond Angles			
Cl–Ru–P1	85.1(1)	P1–Ru–P2	92.6(1)
P1–Ru–C32	103.3(2)	Cl–Ru–C33	131.3(2)
P2–Ru–C33	142.8(2)	Cl–Ru–C34	163.0(2)
Cl–Ru–P2	85.9(1)	P2–Ru–C32	163.8(2)

Conclusion

A general, facile synthetic route to neutral and cationic phosphine ligated ruthenium(II) complexes **7** and **9**, respectively, has been described. The former class of complex is particularly interesting from a structural point of view due to the monodentate ligation of the trifluoroacetate groups to the metal center and the complexes were tested as catalysts for the hydrogenation of olefinic substrates, achieving rather disappointing enantioselectivities. Already described Ru(II) complexes incorporating axial chiral C₂ diphosphine ligands,^{1,2} or related Rh(I) derivatives,^{1a,10a} are without doubt the systems of choice for optimal stereospecificity and efficiency in such hydrogenation reactions.

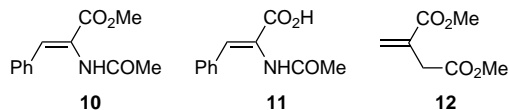
Experimental Section

General Considerations. All reactions with air- or moisture-sensitive materials were carried out under Ar using standard Schlenk techniques. Freshly distilled, dry, and oxygen-free solvents were used throughout. $[\text{Ru}_2(\text{CF}_3\text{CO}_2)_4(\text{H}_2\text{O})(\text{COD})_2]$,¹² $[\text{RuCl}_2(p\text{-cymene})]_2$,²² $[\text{RuCl}_2(\text{COD})]_m$,²³ **3b** and **4b** (abbreviated as (*S,R*)- or (*R,S*)-PPFPh₂),²⁴ and the ferrocenes of the type (*S,R*)- or (*R,S*)-PPFR^{1R}² were prepared according to literature procedures.^{10,11,24} Routine ¹H (250.133 MHz) and ³¹P NMR (101.26 MHz) spectra were recorded with a Bruker AC 250 spectrometer. Chemical shifts are given in ppm and coupling constants (*J*) are given in hertz. Optical rotations were measured with a Perkin-Elmer 341 polarimeter

(22) Bennet, M. A.; Smith, A. *J. Chem. Soc., Dalton Trans.* **1974**, 233.

(23) Albers, M. O.; Ashworth, T. V.; Oosthuizen, E.; Singleton, E. *Inorg. Synth.* **1990**, 26, 69.

(24) Hayashi, T.; Mise, T.; Fukushima, M.; Nagashima, M. K. N.; Hamada, Y.; Matsumoto, A.; Kawakami, S.; Konishi, M.; Yamamoto, K.; Kumada, M. *Bull. Chem. Soc. Jpn.* **1980**, 53, 1151.

Table 4. Hydrogenation of 10–12 Catalyzed by [Ru(CF₃CO₂)₂S₂(PP)] and [RuCl(*p*-cymene)(PP)]PF₆^a

entry	cat. or PP	substrate	solvent	time (h)	yield (%)	ee (%) (config)
1	7a	10	CH ₂ Cl ₂	21	75	69 (S)
2	7a	10	MeOH	20	100	24 (S)
3	7a^b	10	CH ₂ Cl ₂	28	100	29 (S)
4	7a	11	THF/CH ₂ Cl ₂ ^d	20	100	47 (S)
5	7a	11	MeOH	20	100	3 (S)
6	7a^c	11	MeOH	0.5	100	40 (S)
7	7a^c	11	THF/CH ₂ Cl ₂ ^d	45	100	63 (S)
8	7a	12	CH ₂ Cl ₂	17	100	32 (R)
9	7b	10	CH ₂ Cl ₂	90	100	2 (S)
10	7b	10	CH ₂ Cl ₂	15	27	13 (S)
11	7b	12	CH ₂ Cl ₂	20	100	22 (S)
12	7c	10	CH ₂ Cl ₂	18	34	11.3 (S)
13	7c	10	MeOH	0.1	100	7 (R)
14	5b	10	CH ₂ Cl ₂	19	85	75 (R)
15	5b	10	MeOH	19	100	31 (R)
16	5b	12	CH ₂ Cl ₂	19	100	42 (R)
17	5b	12	MeOH	18	100	0
18	5b	10	CH ₂ Cl ₂	16	100	65 (R)
19	5b	11	CH ₂ Cl ₂	20	100	21 (R)
20	5c	10	CH ₂ Cl ₂	21	29	57 (R)
21	5c	10	MeOH	4	100	30 (R)
22	4b	10	CH ₂ Cl ₂	19	67	5.6 (R)
23	4c	10	CH ₂ Cl ₂	66	100	5.9 (S)

^a Reaction conditions: p(H₂) 50 bar; Substrate/Ru = 50 (entries 1–13, 22, and 23); substrate/Ru = 100 (entries 14–21). For all reactions, [substrate] = 1.5–2.5 mmol; room temperature. ^b NEt₃/Ru, 10 equiv. ^c NEt₃/Ru, 50 equiv. ^d 5:4 ratio.

using 10 cm cells. Elemental analyses were performed by the Mikroelementar-analytisches Laboratorium der ETH and by the Analytical Research Services at Ciba-Geigy. Mass spectra were carried out at the Mass Spectroscopy Service of the ETH. Catalytic experiments and analyses of reaction products were carried out as previously described.¹⁰

[Ru(CF₃CO₂)₂(MeOH)₂(2*S*,4*S*-BDPP)] (7a). A solution of **1** (254 mg, 0.57 mmol), in CH₂Cl₂ (3 mL), was slowly added to an orange MeOH solution (6 mL) of [Ru₂(CF₃CO₂)₄(H₂O)-(COD)]₂ (**6**; 252 mg, 0.28 mmol) at room temperature. After 4 h stirring, the resulting red solution was concentrated *in vacuo* to 2 mL, affording **7a** as a yellow powder. Washing with cold MeOH, followed by drying *in vacuo*, gave analytically pure **7a** (yield 359 mg, 75%), which was used as such for the ensuing hydrogenation reactions: [α]_D²⁰ = 90.3 (*c* = 0.6, MeOH); ¹H NMR (CDCl₃, 298 K) δ 7.70–6.70 (m, 20 H, 2 PPh₂), 3.12 (s, 6H, MeOH), 2.94 (m, 1H, PCH), 2.00 (tt, 2H, ³J(HH) = 5.4, ³J(HP) = 20.5, CH₂), 0.94 (dd, 6H, ³J(HH) = 7.0, ³J(HP) = 13.3, 2 Me); ³¹P{¹H} NMR (CDCl₃, 298 K) δ 62.7 (s, PPh₂). Anal. Calcd for C₃₅H₃₈O₆F₆P₂Ru: C, 50.55; H, 4.61. Found: C, 50.50; H, 4.50.

[Ru(CF₃CO₂)₂(MeOH)₂(4*S*,5*S*-DIOP)] (7b). This was prepared as described above for complex **7a** except that **2** (396 mg, 0.79 mmol) and **6** (348 mg, 0.39 mmol) were used: yield 521 mg, 75%; [α]_D²⁰ = 16.3 (*c* = 0.3, CHCl₃); ¹H NMR (CDCl₃, 298 K) δ 7.50–7.30 (m, 20 H, 2 PPh₂), 3.86 (m, 1H, CH), 2.97 (s, 6H, MeOH), 2.93 (m, 1H, PCH), 2.50 (m, 1H, PCH), 1.29 (s, 6H, 2 Me); ³¹P{¹H} NMR (CDCl₃, 298 K) δ 45.4 (s, PPh₂). Anal. Calcd for C₃₇H₄₀O₈F₆P₂Ru: C, 49.95; H, 4.53. Found: C, 49.80; H, 4.44.

[Ru(CF₃CO₂)₂(EtOH)₂-(*R*)-(S)-PPFCy₂)] (7c). This was prepared as described above for complex **7a** except that **4a** (196 mg, 0.33 mmol) and **6** (146 mg, 0.165 mmol) were used and that ethanol was employed as solvent: yield 135 mg, 80%; ¹H NMR (CDCl₃/CD₃OH, 298 K) δ 7.78–7.70 (m, 10 H, PPh₂), 4.62, 4.54, 4.40 (3s, 3H, C₅H₃), 3.65 (q, 2H, ³J(HH) = 7.0, CH₂), 3.35 (m, 1H, PCH), 3.54 (s, C₅H₅), 1.76 (dd, 3H, ³J(HP) = 10.2,

³J(HH) = 7.4, Me), 1.21 (t, 3H, ³J(HH) = 7.0, CH₂Me), 2.37–0.86 (m, 22H, Cy); ³¹P{¹H} NMR (CDCl₃/CD₃OH, 298 K) δ 45.4 (s, PCy₂). Anal. Calcd for C₄₄H₅₆F₆FeO₆P₂Ru: C, 52.13; H, 5.57. Found: C, 52.35; H, 5.68.

[Ru(CF₃CO₂)₂(MeOH)₂(PPFPhCy)] (7d). This was prepared as described above for complex **7a** except that **5a** (96 mg, 0.16 mmol) and **6** (72 mg, 0.08 mmol) were used: yield 98 mg, 61%; ¹H NMR (CDCl₃/CD₃OH, 298 K) δ 7.87–7.79 (m, 15 H, PPh), 4.62, 4.28, 3.86 (3s, 3H, C₅H₃), 3.60 (s, 5H, C₅H₅), 3.35 (m, 1H, PCH), 1.83 (dd, 3H, ³J(HP) = 11.4, ³J(HH) = 7.3, Me), 2.45–1.34 (m, 11H, Cy); ³¹P{¹H} NMR (CDCl₃/CD₃OH, 298 K) δ 68.61 (d, ²J(PP) = 50.4, PPh₂), 53.67 (d, ²J(PP) = 50.4, PCyPh). Anal. Calcd for C₄₂H₅₆F₆FeO₆P₂Ru: C, 51.49; H, 4.73. Found: C, 51.97; H, 4.35.

[RuCl{(S)-(R)-PPFCy₂}(p-cymene)]PF₆ (9a). **3a** (317 mg, 0.53 mmol) and [RuCl₂(*p*-cymene)]₂ (161 mg, 0.26 mmol) were heated in a 3:1 suspension of EtOH/CH₂Cl₂ (15 mL:5 mL) at 60 °C for 1.75 h. After cooling and filtration over Celite to remove some decomposition products, the orange suspension was evaporated to dryness. Metathesis with excess KPF₆ (210 mg, 1.14 mmol) in MeOH (20 mL) for 2 h at room temperature was followed by solvent evaporation. The orange residue was extracted with CH₂Cl₂ (50 mL) and the organic phase washed with water (10 mL) and then dried over MgSO₄. Removal of the latter by filtration followed by evaporation of the filtrate afforded an orange solid: yield 478 mg, 89%; [α]_D²⁰ = 271 (*c* = 0.16, CH₂Cl₂); ¹H NMR (CDCl₃, 298 K) δ 8.25–7.00 (m, 10 H, PPh₂), 6.21 (m, 2H, Hcym), 6.08 (d, 1H, ³J(HH) = 6.0, Hcym), 5.78 (m, 1H, Hcym), 4.97 (dq, 1H, ³J(HH) = 5.4, PCHMe), 4.59, 4.42, 4.35 (3m, 3H, C₅H₃), 4.00 (s, C₅H₅ of minor diastereomer), 3.59 (s, 5H, C₅H₅), 2.77, 2.51, 2.30 (3m, 3H, Me₂CH, 2CH cyclohex), 2.20–0.84 (m, 29H, Cy, MeCHP, CHMe₂), 0.55 (s, 3H, Me); ³¹P NMR δ 53.4 (d, ²J(PP) = 55.8, PCy₂), 25.8 (d, ²J(PP) = 55.8, PPh₂), –144.8 (sept, ¹J(PF) = 713, PF₆). Traces of a second diastereomer at δ = 35 and 54 ppm were detected. MS (FAB) 865 (M⁺, 15). Anal. Calcd for C₄₆H₅₈ClF₆FeP₃Ru: C, 54.69; H, 5.79. Found: C, 54.97; H, 6.04.

[RuCl{(R)-(S)-PPFCy₂}(p-cymene)]PF₆ (9a'). This was made in a fashion analogous to its (*S*)-(*R*) derivative: [α]_D²⁰ = –233 (*c* = 0.25, CH₂Cl₂).

[RuCl{(S)-(R)-PPFPh₂}(p-cymene)]PF₆ (9b). This was made in a fashion analogous to **9a** using **3b** (118 mg, 0.20 mmol) and [RuCl₂(*p*-cymene)]₂ (60 mg, 0.10 mmol), followed by metathesis with KPF₆ (74 mg, 0.40 mmol) in MeOH, and obtained as an orange solid: yield 144 mg, 72%; [α]_D²⁰ = 213 (*c* = 0.45, CH₂Cl₂); ¹H NMR (CDCl₃, 298 K) δ 8.28–6.90 (m, 20H, 2 PPh₂), 6.03, 5.81, 5.57, 4.55 (4m, 4H, Hcym), 5.22 (dq, 1H, ³J(HH) = 5.4, PCHMe), 4.48, 4.33, 4.30 (3m, 3H, C₅H₃), 4.04 (s, C₅H₅ of minor diastereomer), 3.68 (s, 5H, C₅H₅), 2.64 (q, 1H, ³J(HH) = 5.6, CHMe₂), 1.45 (ABX, 3H, ³J(HH) = 6.9, ³J(HP) = 13.4, PCHMe), 1.25, 0.77 (2d, 6H, ³J(HH) = 6.5, CHMe₂), 0.63 (s, 3H, Me); ³¹P NMR δ 48.3 and 27.4 (d, ²J(PP) = 58, PPh₂), –144.8 (sept, ¹J(PF) = 713, PF₆); second isomer (~16%) at δ 54.8, 37.2 (2d, ²J(PP) = 58, PPh₂). MS (FAB) 853 (M⁺, 100). Anal. Calcd for C₄₆H₄₆ClF₆FeP₃Ru: C, 55.35; H, 4.65. Found: C, 55.23; H, 4.56.

[RuCl{(S)-(R)-PPFPhobyl}(p-cymene)]PF₆ (9c). This was made in a fashion analogous to **9a** using **3c** (139 mg, 0.26 mmol) and [RuCl₂(*p*-cymene)]₂ (79 mg, 0.13 mmol), followed by metathesis with KPF₆ (92 mg, 0.5 mmol) in MeOH, and obtained as a pale brown solid: yield 191 mg, 77%; [α]_D²⁰ = 77 (*c* = 0.1, CH₂Cl₂); ¹H NMR (CDCl₃, 298 K) δ 7.70–7.25 (m, 10 H, PPh₂), 6.22, 5.81, 5.42, 5.24 (4m, 4H, Hcym), 4.52, 4.40, 4.07 (3m, 3H, C₅H₃), 4.01 (s, 5H, C₅H₅ of minor diastereomer), 3.87 (s, 5H, C₅H₅), 3.73 (m, 1H, PCHMe), 2.78 (m, 1H, CHMe₂), 2.40–0.80 (m, 17H, Hphob, Me), 1.08, 1.00 (2d, 6H, ³J(HH) = 6.1, Me₂CH); ³¹P NMR δ 35.4 (m), 29.0 (d, ²J(PP) = 57, PPh₂), –144.8 (sept, ¹J(PF) = 713, PF₆). MS (FAB) 809 (M⁺, 11). Anal. Calcd for C₄₂H₅₀ClF₆FeP₃Ru: C, 52.87; H, 5.28. Found: C, 51.78; H, 5.62.

[RuCl{(S)-(R)-PAsFCy₂}(p-cymene)]PF₆ (9d). This was made in a fashion analogous to **9a** except using **3d** (125 mg, 0.20 mmol) and [RuCl₂(*p*-cymene)]₂ (56 mg, 0.09 mmol),

followed by metathesis with KPF_6 (97 mg, 0.53 mmol) in MeOH, and obtained as an orange solid: yield 170 mg, 82%; $[\alpha]_D^{20} = 169$ ($c = 0.4$, CH_2Cl_2); $^1\text{H NMR}$ (CDCl_3 , 298 K) δ 8.04–7.10 (m, 10 H, PPh_2), 6.22 (d, 1H, $^3J(\text{HH}) = 5.1$, Hcym), 6.07, 5.72 (2d, 2H, Hcym), 4.68 (dq, 1H, $^3J(\text{HH}) = 6.5$, PC^iMe), 4.59, 4.44, 4.37 (3m, 3H, C_5H_3), 3.99 (s, 5H, C_5H_5 of minor diastereomer), 3.63 (s, 5H, C_5H_5), 2.75–0.83 (m, 31H, Cy, MeCHP , CHMe_2), 0.74 (s, 3H, Me); $^{31}\text{P NMR}$ δ 48.8 (s, PCy_2), -144.8 (sept, $^1J(\text{PF}) = 713$, PF_6). MS (FAB) 909 (M^+ , 22). Anal. Calcd for $\text{C}_{46}\text{H}_{58}\text{AsClF}_6\text{FeP}_2\text{Ru}$: C, 52.41; H, 5.55. Found: C, 51.81; H, 5.40.

Acknowledgment. The Swiss National Science Foundation (CHiral2 program, Grant 2127-41'203.94)

is gratefully acknowledged (by J.S.) for financial support of this project. V. Gramlich is thanked for solving the structure of **9a**.

Supporting Information Available: Tables of crystal data and refinement details, atomic coordinates, complete listing of bond distances and angles, torsion angles, tables of anisotropic displacement coefficients, and positional parameters for **7a**, **7b**, **7c**, and **9a'** (51 pages). Ordering information is given on any current masthead page. Tables of calculated and observed structure factors for all four compounds (167 pages) may be obtained from the authors upon request.

OM9506781